

Ultrafast Voltage Sampling using Single-Electron Wavepackets

N. Johnson,^{1,2,*} J. D. Fletcher,¹ D.A. Humphreys,¹ P. See,¹ J.P. Griffiths,³ G.A.C. Jones,³ I. Farrer,^{3,†} D.A. Ritchie,³ M. Pepper,² T.J.B.M Janssen,¹ and M. Kataoka^{1,‡}

¹*National Physical Laboratory, Hampton Road,
Teddington, Middlesex TW11 0LW, United Kingdom*

²*London Centre for Nanotechnology,
and Department of Electronic and Electrical Engineering,
University College London, Torrington Place,
London, WC1E 7JE, United Kingdom*

³*Cavendish Laboratory, University of Cambridge,
J.J. Thomson Avenue, Cambridge CB3 0HE, United Kingdom*

(Dated: May 10, 2022)

Abstract

We demonstrate an ultrafast voltage sampling technique using a stream of single-electron wavepackets. Electrons are emitted from a semiconductor single-electron pump and travel through electron waveguides towards a detector potential barrier. A reference DC voltage and test AC waveform are added onto a surface gate to form the detector barrier. Our electrons sample an instantaneous voltage on the gate upon arrival at the detector barrier. Fast sampling is achieved by minimising the duration that the electrons interact with the barrier, which can be made as small as a few picoseconds. The value of the instantaneous voltage can be determined by varying the reference DC voltage to match the barrier height with the electron emission energy, which is used as a stable reference. The test waveform can be reconstructed by shifting the electron arrival time against it. We argue that this method has scope to increase the bandwidth of voltage sampling to 100 GHz and beyond.

There is much interest in producing faster electronic devices for high-performance computing and large-volume data communication. High frequency signal analysis becomes important in the testing and design of these high speed applications. Sampling oscilloscopes employ a sampling gate created by a switch that when closed, permits the input signal to propagate into the sampling circuit. The bandwidth of commercial sampling oscilloscopes using this principle are approaching 100 GHz. The limiting factor to their bandwidth is largely due to parasitic capacitance in the components and across the switch. While it is in principle straightforward to sample at very high rates, by producing short pulses to close the switch, parasitic loss increases with frequency¹.

One radical approach to such a problem may be to use a short wavepacket of a single quasiparticle (e.g. a conduction band electron) instead of a voltage pulse. The information transmitted by quasiparticle wavepackets (wavefunctions) is protected in the absence of scattering or tunneling events. The use of a wavefunction as the media of (classical) information transfer allows us to achieve high-speed device operations without the bandwidth limitations imposed by conventional waveguides.

In this letter, we present an ultrafast voltage sampling method using single-electron wavepackets traveling through electron waveguides in a semiconductor substrate. An unknown AC test signal is added to a control DC voltage on to a gate to form a potential barrier in the path of the electron wavepackets. The transmission probability through the barrier depends on the instantaneous barrier height on arrival at the detector relative to the electron energy. In this manner, our electrons can sample the test signal voltage, in a similar way to the sample and hold method using a voltage comparator in conventional sampling oscilloscopes. High bandwidth of this sampling is achieved by tuning the electron's arrival-time distribution to 10 picoseconds or shorter. Our method in principle eliminates the bandwidth limitation that plagues conventional electronic devices. While the present experiment is limited by the bandwidth of the transmission line of the test signal, we argue that this method has the potential to increase the bandwidth of voltage sampling up to 100 GHz and beyond.

The principle of our scheme is presented in Figs. 1(a) - (c). Single electron wavepackets are generated at a fixed energy and travel one by one along the same path towards a potential barrier, which we call the detector barrier. The direction the wavepackets travel on arrival at the detector barrier depends on the barrier height, which is controlled by a gate voltage.

If the electrons have an energy greater than the potential on this barrier, they pass through it. If the electrons do not have enough energy, they are deflected by the barrier. This path direction is only dependent on the instantaneous barrier potential at *the time of electron arrival*. The electrons do not interact with the barrier when they are not at the site of the barrier. Therefore, we can use this information to sample the gate voltage at a very short timescale.

We initially apply a detector gate voltage such that the barrier is held at half transmission (Fig. 1(a))². At this voltage, each electron wavepacket has a $\sim 50\%$ probability of tunneling through the detector potential. We denote this threshold voltage the “REFERENCE”. When we add a test signal to the detector gate, the transmission of wavepackets either increases or decreases, depending on the sign of the test signal (Fig. 1(b)(i) and (ii)). We then add a further DC voltage to the detector gate, which we call the OFFSET (Fig. 1(c)). If the magnitude of this offset voltage exactly matches that of the instantaneous test signal, but with the opposite sign, then the barrier is brought back to the original point of half transmission. This way, we can “sample” the instantaneous value of the test signal.

This method can be compared to that of voltage sampling by a sample and hold method^{1,3}. The simplified block diagrams for the sample and hold method and our method are compared in Fig. 1(d). In the sample and hold method, a trigger pulse closes a switch which permits the test signal to propagate onto a capacitor. When the switch is opened, the voltage is measured by the comparator⁴. This allows a fast waveform to be sampled by the capacitor taking “snapshots” of the waveform each time it is charged. In our method, our single-electron wavepackets represent trigger pulses. The voltage comparison is made between the test signal and applied DC offset voltage (with opposite signs). The comparison voltage of the sample and hold method is equivalent to the offset voltage of our method. Very fast voltage sampling is possible with this method, because the timescale of sampling is determined by the length of electron wavepackets, or more precisely, their arrival-time distribution at the potential barrier. This can be easily made to be on the order of picoseconds⁵. The waveform of the test signal can be scanned by shifting the electron arrival time against it to sample different parts of the waveform. In principle, our method should work in single-shot mode, in which we could use a charge sensor to record the transmission of a single electron across the detector barrier. Although technologically plausible, we do not yet have such detection capability. Here, as a demonstration of proof of principle, we use a periodic test signal, to

which the timing of electron wavepacket injection is synchronised. This way, the direction of electron flow can be detected as a current.

Fig. 1(e) shows a schematic of the device and connections used to realise our sampling scheme. A GaAs/AlGaAs heterostructure defines a two dimensional electron gas (2DEG) ~ 90 nm below the surface. The active area of the device is etched to confine the 2DEG to a $1.5 \mu\text{m}$ -wide channel (grey shading). Ti-Au metallic gates G_1 , G_2 and G_D are patterned on the surface using electron beam lithography. Gates G_1 and G_2 define the quantum dot single-electron pump that is our source of fixed energy electron wavepackets⁶⁻¹⁰. The quantum dot is defined as a circular cut out of radius 150 nm between the gates. Gate G_D acts as the detector barrier, and lies $4 \mu\text{m}$ away from the pump. Experiments are performed in a cryostat with a base temperature ~ 300 mK and with a magnetic field of 14 T applied perpendicular to the plane of the 2DEG.

The electron pump is operated so that it emits electrons one by one at a stable fixed energy ~ 100 meV above the Fermi energy¹¹. The typical broadening of the emission energy (taken as the full width at half maximum of the transmission profile across the detector, dI_d/dVG_{GD}^{DC}) is ~ 4 meV. This sets the voltage resolution of our scheme, at approximately 2 mV. G_1 is driven by an AC sinusoidal waveform at 240 MHz with peak-to-peak amplitude ~ 1 V from one channel of an arbitrary waveform generator (AWG). During the pump cycle, electrons populate the quantum dot, and are then ejected from it over the drain barrier G_2 . This produces a quantised current $I = ef$, with e the elementary charge and f the frequency of the driving waveform. In the presence of a sufficient perpendicular magnetic field, the ejected electrons travel along the sample edge, in a similar manner to the edge-state transport in the quantum Hall regime¹², but as hot electrons in the states higher than the Fermi energy (marked as red paths in Fig. 1(e)). No appreciable energy loss occurs between the pump and the detector G_D due to the long scattering length in the edge states, which is of order tens of microns^{9,13}. A test signal is applied to the detector from the second channel of the AWG, synchronised to the pump signal from the first channel (although in principle any synchronised RF source could be used). We place our measurement ammeter on the contact behind the detector (see Fig. 1(e)) so it will record the the transmitted current, which is a measure of the detector barrier transmission. We set the reference, V_{GD}^{DC} , and offset, ΔV_{GD}^{DC} , voltages to the detector as per the scheme in Fig. 1(a) - (c), and use the change in the transmitted current as a readout. By tracking the change in voltage of the

half transmission point by adjusting the offset, we deduce the amplitude of the test waveform at the instantaneous sampling interval. For this work, we use a Tektronix AWG7122C as our AWG. Our pump drive and test waveforms are constructed with a 50 point sine wave at a sampling rate of 12 GS/s, giving us a 240 MHz signal. The pump drive signal and, for this first test the detector test signal, are filtered using a 630 MHz low pass filter. Although we used the same frequency for the pump drive and the test signal, the necessary condition for this scheme to work is only that the frequency of the test signal must be exactly an integer multiple of the pump drive frequency. The electron pump has been shown to operate over a wide frequency range, increasing the range of measurable frequencies of test signals⁶. Below ~ 100 MHz the pump does not output a large enough current to accurately measure, and above ~ 1 GHz it loses accuracy, making it an unreliable source.

Fig. 2(a) shows how we can sample the test waveform at different times to build up its temporal form. There exists an time delay, t_d , between the test waveform V_{GD}^{AC} , and the pump driving waveform V_{G1}^{AC} . Changing this delay by a quantity Δt_d allows us to control the arrival time of the electrons at the detector. Electrons will then sample a different part of the test waveform on arrival at the detector barrier. We can control Δt_d with 1 picosecond resolution, using the internal skew control between the two output channels of the AWG7122C. Because the electron arrival time distribution is so short compared to the timescale that our test waveform voltage changes, we can consider the test waveform to be quasi-static in the sampling time.

Fig. 2(b) is an example result, plotting in the colour scale the derivative of the measured current with respect to the detector barrier offset voltage, $dI_D/d\Delta V_{GD}^{DC}$. In this measurement our test signal is a sine wave. The vertical axis is the offset voltage, centered about zero, and the horizontal axis is the set time delay between the pump drive signal and the test waveform, Δt_d . We plot the derivative of the current with respect to the detector gate voltage, $dI_D/d\Delta V_{GD}^{DC}$ (i.e. vertically in Fig. 2(b)), to show the onset of barrier transmission with greater clarity. To examine the validity of this method, we compare the experimental data points against a true sine curve in Fig. 2(c). They match well within the voltage resolution of the offset voltage, showing that this measurement has a good linearity between electron energy and V_{GD}^{DC} .

The results mentioned above demonstrate the basic principle of voltage sampling using single-electron wavepackets. We now explore the bandwidth limitation of this method. In

order to do this, we remove the filter from the test-signal line, so that the distortion by higher harmonics from the AWG transmit to the detector gate. The AWG construction of a sinusoidal waveform is shown in Fig. 3(a), and the resultant current map in Fig. 3(b), again plotted with the derivative of current in the colourscale for clarity, as in Fig. 2(b). Again, as in Fig. 2(c), we extract the peak in the derivative in Fig. 3(c). We note that we recover the overall shape of the waveform, but that there are additional features, principally a higher frequency oscillation, dominated by 12 GHz components, the zeroth harmonic of the AWG's sampling rate.

We now investigate this oscillation and show it is not due to the electron properties or pump instability. Deviations from the true sine wave seen here are not due to measurement noise, but are due to harmonics from the AWG causing small oscillations superimposed on to the signal. To demonstrate that these features are not experimental artifact, we used a Tektronix MSO72304DX Mixed Signal Oscilloscope, with 23 GHz bandwidth, at the end of the measurement probe (taken out from the cryostat, and sample removed) where the device is connected at room temperature (with an extra 1 m of coaxial cable), in order to measure the AWG output signal. The oscilloscope is measuring the waveform as would be seen by the sample, using the same measurement lines. In Fig. 3(c), we compare the oscilloscope trace of the waveform with the extracted waveform from the sample (as performed in Fig. 2(c)), in the red and black traces respectively. We note that the oscilloscope measurement has an amplitude of approximately half the magnitude of our sampling scheme, owing to it not being an open ended measurement. In Fig. 3(c) we scale the scope trace by factor 2 to make it easier to compare the traces. While the very fine details are different, probably due to the difference between the open ended measurement of our single-electron device and the 50 ohm matched measurement of the MSO, there is sufficient similarity to assume that our device faithfully measures the voltage signal. For Figs. 3 (d) - (f), we repeat the measurement analysis performed on the sine wave for an unfiltered square wave. The sharpness of the step of the square wave observed in our sample, as seen in Fig. 3(f), implies high bandwidth of this measurement method.

To more quantitatively demonstrate our bandwidth, we compare it to the bandwidth of the oscilloscope. To do this, we use a fast waveform and compare the harmonic components between the oscilloscope and our sample. We use the two-point construction as shown in Fig. 4(a), at a frequency of 6 GHz, and proceed to analyse our measurement in the same way

as Fig. 3, obtaining the current measurement map in Fig. 4(b), and the peak extraction in Fig. 4(c). As before, the oscilloscope measurement is taken with the instrument connected to the measurement probe, removed from the cryostat. Fig. 4(c) shows there is a small difference in attenuation of higher frequency components which gives us the slightly differing waveform shapes. We take the Fast Fourier Transform (FFT) of both traces, and plot them in Fig. 4(d). There is one notable difference - the oscilloscope records an 18 GHz component which is not seen on our sample. Another way of measuring the bandwidth of our method is to examine the arrival time distribution of the electrons at the detector barrier, as shown in Fig. 4(e). This distribution is a measure of the size of the temporal projection of the single electron wavepacket (with experimental broadening)⁵. We take the full width at half maximum of a Gaussian fit as the upper limit to our wavepacket temporal projection size, and we find this to be 14 ps. This should give us a temporal resolution of approximately 28 ps, or a bandwidth of 35.7 GHz. We speculate that our bandwidth limitation is due to the transmission line on the sample holder and on chip. This accounts for the FFT of Fig. 4(d) not having an 18 GHz peak in the transmission. This is also supported by the peak at 12 GHz having a larger amplitude for the sample: we speculate that the signal transmission in our experimental line is flat up to ~ 12 GHz compared to the sampling scope, but drops sharply above this frequency. If these are improved, and high frequency signals can be applied onto the detector gate, we should be able to achieve a very large bandwidth. Additionally, more recent work on the temporal wavepacket size has indicated that with careful tuning of the pump operating point, it is possible to find a wavepacket size of less than 10 ps^{14,15}. This opens the possibility of bandwidths in excess of 50 GHz, and speculatively in excess of 100 GHz.

To summarise, we have demonstrated a technique of using single electron wavepackets to sample an unknown AC waveform, in a method similar to that employed in a sampling oscilloscope with the possibility of realising a bandwidth in excess of 100 GHz. Other than the high-bandwidth applications, one area which this method can be useful is in-situ voltage waveform measurements in a cryogenic environment. On chip signal verification is becoming increasingly needed for fine control of quantum systems, for example in qubit state initialisation¹⁶. Whilst there exists a method of using qubits themselves to do this, it has limitations to some signal forms¹⁶. We propose that our system would be more generally usable in such applications, as a way of verifying the precise shape of signals on chip, and

opens up the possibility of quantum measurements through precise signal control.

We thank John Marrinan, Chris Skach, and James Niblock from Tektronix for useful discussions on AWG and sampling oscilloscope technologies. We also thank Stephen Giblin for useful discussions. This research was supported by the UK Department for Business, Energy, and Industrial Strategy and by UK EPSRC.

* nathan.johnson@npl.co.uk

† Present address: Department of Electronic and Electrical Engineering, University of Sheffield, Mappin Street, Sheffield S1 3JD, United Kingdom

‡ masaya.kataoka@npl.co.uk

¹ T. H. O'Dell, *Circuits for Electronic Instrumentation* (Cambridge University Press, 1991).

² We take the point of maximum derivative of the current with respect to the detector dI_D/dV_{GD}^{DC} as our half transmission point. The point of maximum derivative may not occur at exactly half transmission, but this does not compromise our method. In all samples tested the discrepancy was found to be small.

³ J. M. D. Pereira, *IEEE Instr. Meas. Mag.* 9 27 (2006).

⁴ In Fig. 1(d), we use a simple semiconductor switch to show a fast acting switch in the oscilloscope circuit, but acknowledge that real architectures will not employ this switching method, due to leakage in the open state.

⁵ J. Waldie, P. See, V. Kashcheyevs, J. Griffiths, I. Farrer, G. Jones, D. Ritchie, T. Janssen, and M. Kataoka, *Phys. Rev. B* 92, 125305 (2015).

⁶ S. P. Giblin, M. Kataoka, J. D. Fletcher, P. See, T. J. B. M. Janssen, J. P. Griffiths, G. A. C. Jones, I. Farrer, and D. A. Ritchie, *Nature Comms.* 1935 (2012).

⁷ C. Leicht, P. Mirovsky, B. Kaestner, F. Hohls, V. Kashcheyevs, E. V. Kurganova, U. Zeitler, T. Weimann, K. Pierz, and H. W. Schumacher, *Semicond. Sci. Tech.* 26 055010 (2011).

⁸ M. D. Blumenthal, B. Kaestner, L. Li, S. Giblin, T. J. B. M. Janssen, M. Pepper, D. Anderson, G. Jones, and D. A. Ritchie, *Nature Phys.* 3 343 (2007).

⁹ J. D. Fletcher, M. Kataoka, S. P. Giblin, S. Park, H.-S. Sim, P. See, D. A. Ritchie, J. P. Griffiths, G. A. C. Jones, H. E. Beere, and T. J. B. M. Janssen, *Phys. Rev. B* 86 155311 (2012).

¹⁰ B. Kaestner, V. Kashcheyevs, G. Hein, K. Pierz, U. Siegner, and H. W. Schumacher, *App.*

Phys. Lett. 92 192106 (2008).

- ¹¹ J. D. Fletcher, P. See, H. Howe, M. Pepper, S. P. Giblin, J. P. Griffiths, G. A. C. Jones, I. Farrer, D. A. Ritchie, T. J. B. M. Janssen, and M. Kataoka, Phys. Rev. Lett. 111 216807 (2013).
- ¹² B. I. Halperin, Phys. Rev. B 25 2185 (1982).
- ¹³ D. Taubert, C. Tomaras, G. J. Schinner, H. P. Tranitz, W. Wegscheider, S. Kehrein, and S. Ludwig, Phys. Rev. B 83, 235404 (2011).
- ¹⁴ M. Kataoka, J. D. Fletcher, and N. Johnson, to be submitted to Physica Status Solidi (2016).
- ¹⁵ (2016), we will publish details of this elsewhere.
- ¹⁶ M. Hofheinz, H. Wang, M. Ansmann, R. C. Bialczak, E. Lucero, M. Neeley, A. D. OConnell, D. Sank, J. Wenner, J. M. Martinis, and A. N. Cleland, Nature 459 548 (2009).

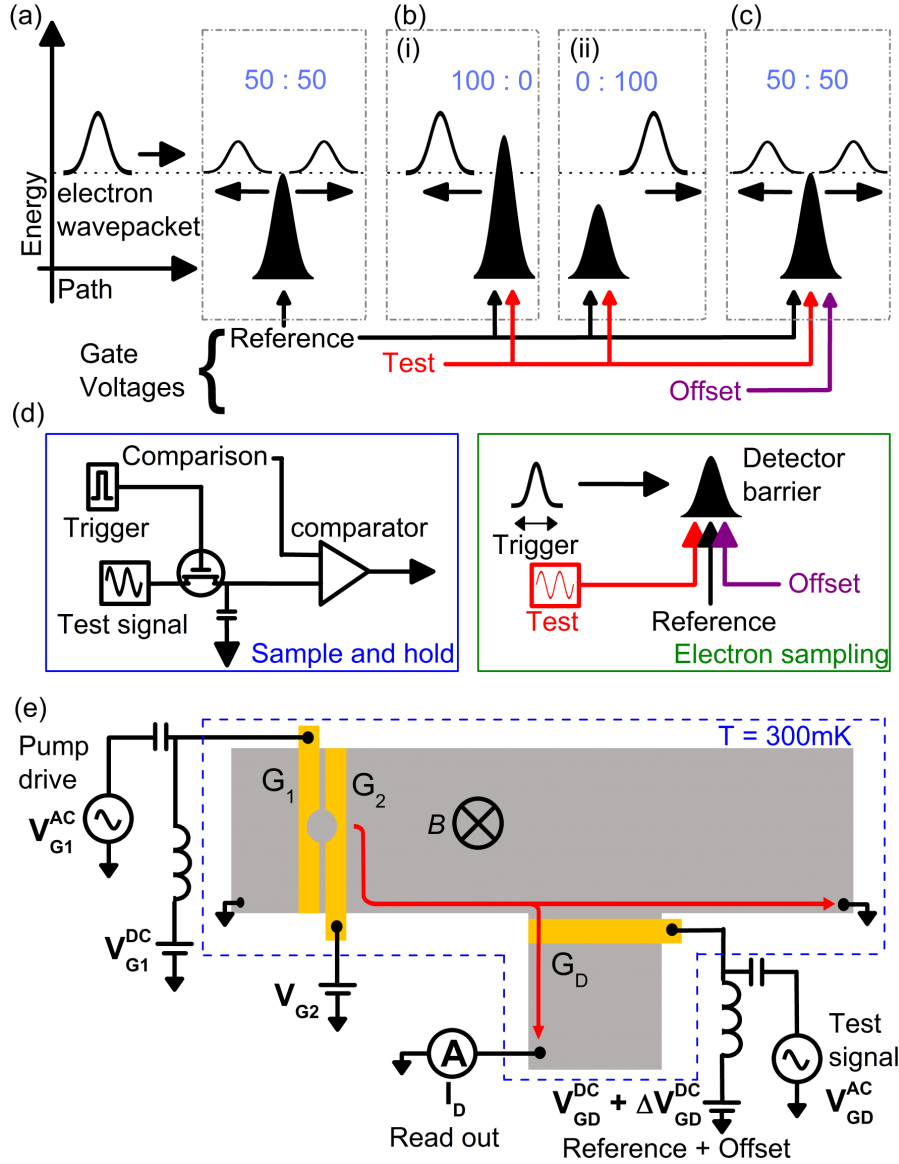


FIG. 1. (a) - (c) Principle of single electron sampling. (a) We find the point at which half transmission across the barrier occurs. This is our reference. (b) When we add the unknown test signal transmission is modified to either fully reflected (i) or fully transmitted (ii) because the total potential on the gate is modified. (c) By adding an offset we return the detector gate potential to the half transmission point. (d) Block diagram comparisons between a sample and hold method and the equivalent methods in our single-electron based oscilloscope. (e) Schematic of the device used. Gates G_1 and G_2 form the electron pump, which produces a source of single electron wavepackets. These propagate across the device in edge states (red) to the detector barrier G_D , which implements the scheme presented in (a) - (c).

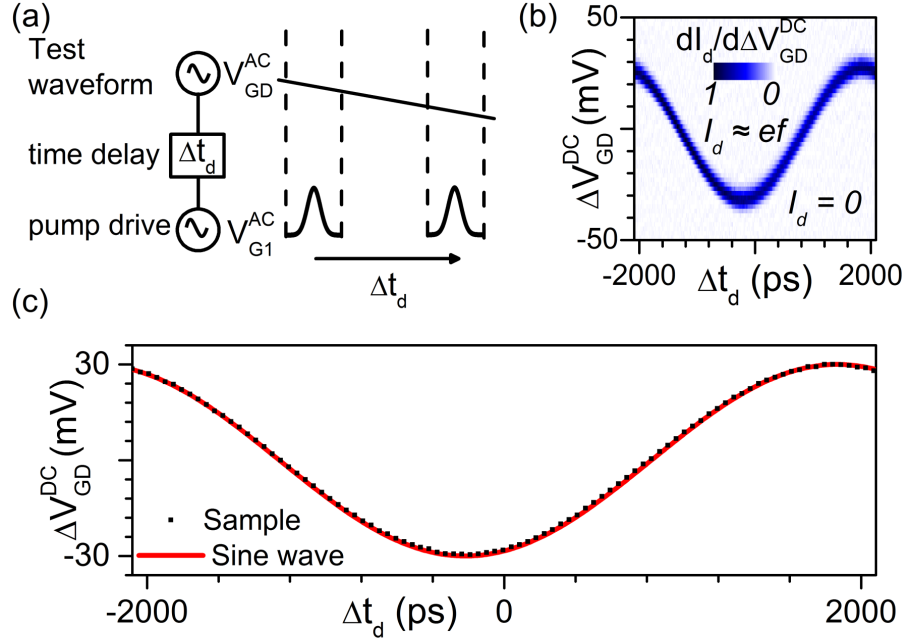


FIG. 2. (a) Changing the time delay, Δt_d , allows the electron wavepacket to sample different parts of the test waveform. The sampling window is limited by the length of the wavepacket in the time domain, hence setting the bandwidth. (b) An example result. We plot the derivative, $dI_D/d\Delta V_{GD}^{DC}$ for clarity of the onset of transmission across the barrier. The test signal has equal amplitude (but opposite sign) to the offset voltage. (c) Extraction of the peak in the derivative from (b) when compared to the expected test waveform shape (red) shows good agreement.

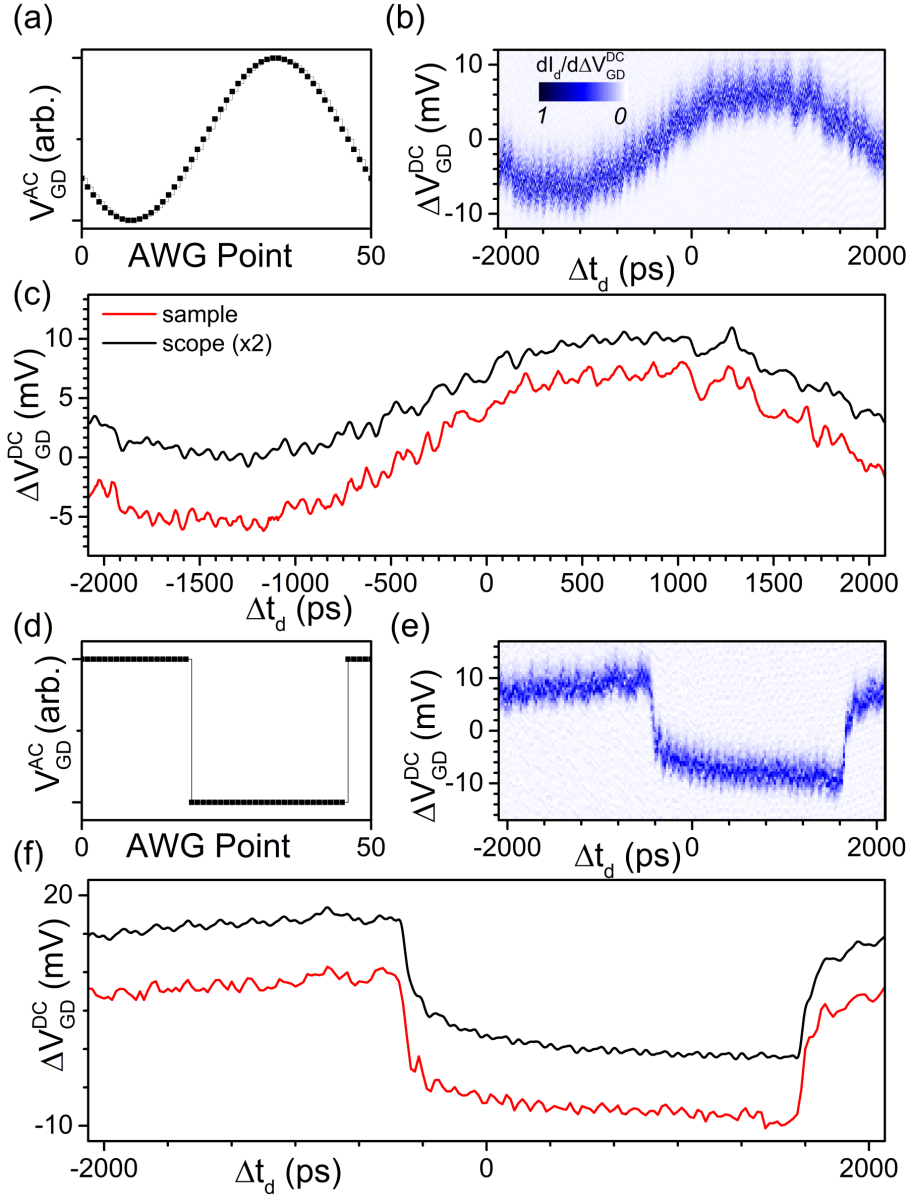


FIG. 3. Application of two waveforms to the detector. (a) The AWG construction of the waveform. (b) The resultant waveform produced by the device, equivalent to Fig. 2(b). (c) The measured waveform shows good agreement when compared to an oscilloscope. (d) - (f) Repeated analysis in the case of a square wave.

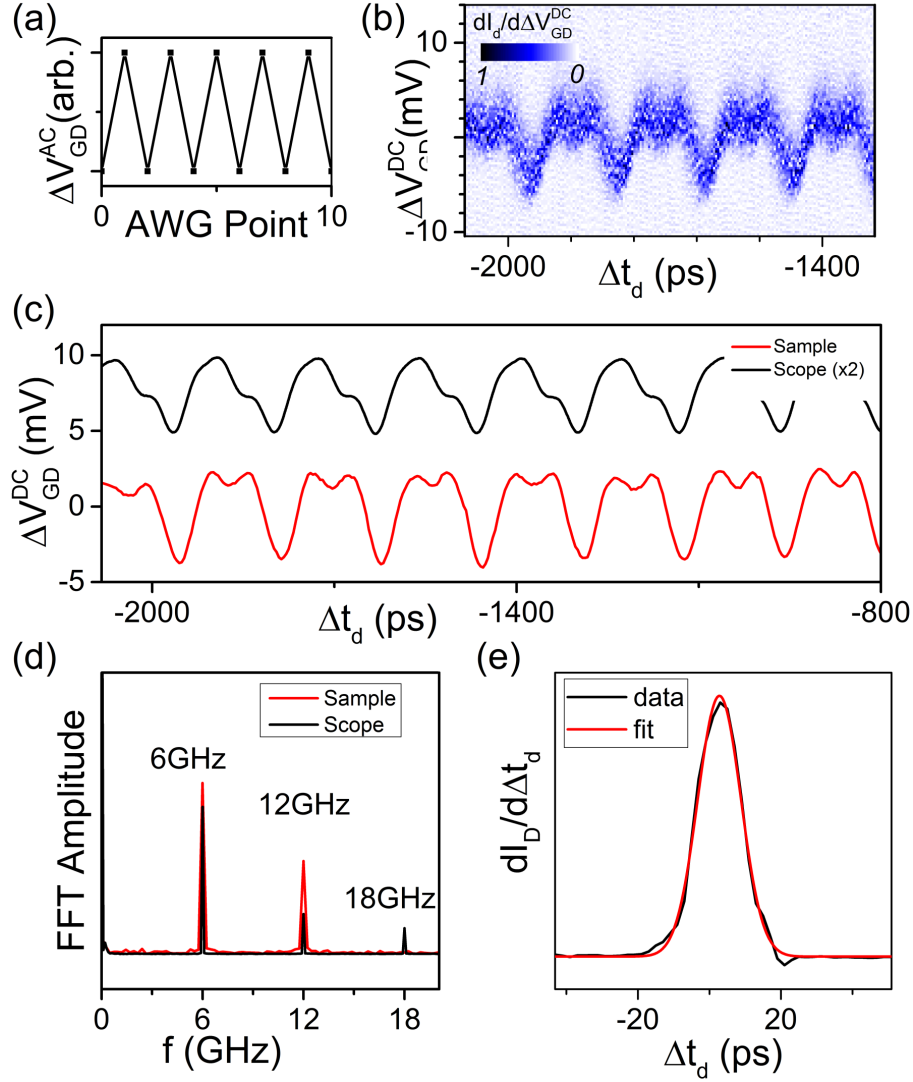


FIG. 4. (a) The AWG construction of a two-point waveform run at 12 GS/s, giving a 6 GHz frequency. (b) The resultant current map as measured by the device, derivative shown for clarity. (c) Comparison between our device measurement and the oscilloscope show no large differences. (d) The Fast Fourier Transforms (FFT) of each signal are comparable, with some attenuation of the highest component on the sample, accounting for the difference between the traces seen in (c). (e) A direct measurement of the bandwidth of our method by analysis of the arrival time distribution at the detector barrier. We deduce a wavepacket size from a Gaussian fit to be 14 ps, giving a potential bandwidth of greater than 30GHz.